Title

Rational Development of Remote C−H Functionalization of Biphenyl: Experimental and Computational Studies

Journal

Angewandte Chemie International Edition, 59(12)

ISSN

1433-7851

Authors

Fan, Zhoulong
Bay, Katherine L
Chen, Xiangyang
et al.

Publication Date

2020-03-16

DOI

10.1002/anie.201915624

Peer reviewed

Published in final edited form as:

Angew Chem Int Ed Engl. 2020 March 16; 59(12): 4770–4777. doi:10.1002/anie.201915624.

Rational Development of Remote C–H Functionalization of Biphenyl: Experimental and Computational Studies

Zhoulong Fan[a,+], **Katherine L. Bay**[b,+], **Xiangyang Chen**[b], **Zhe Zhuang**[a], **Han Seul Park**[a], **Kap-Sun Yeung**[c], **K. N. Houk**[b], **Jin-Quan Yu**[a]

[a]Department of Chemistry, The Scripps Research Institute, 10550 North Torrey Pines Road, La Jolla, CA 92037 (USA)

[b]Department of Chemistry and Biochemistry, University of California, Los Angeles, CA 90095 (USA)

[c]Discovery Chemistry, Bristol-Myers Squibb Research and Development, 100 Binney Street, Cambridge, MA 02142, United States

Abstract

We now report simple and efficient nitrile-directed *meta*-C–H olefination, acetoxylation and iodination of biaryls. Compared to our previous approach of installing a complex U-shaped template to achieve a molecular U-turn and assemble the large sized cyclophane transition state for the remote C–H activation, a synthetically useful phenyl nitrile functional group could also direct remote *meta*-C–H activation. This reaction provides a useful method for modifying biaryl compounds because the nitrile can be readily converted to amines, acids, amides or other heterocycles. Notably, the remote *meta*-selectivity of biphenylnitriles could not be expected from previous results with a macrocyclophane nitrile template. DFT computational studies now show that a ligand-containing Pd–Ag heterodimeric transition state (TS) favors the desired remote *meta*-selectivity. Control experiments demonstrate the directing effect of the nitrile and exclude the possibility of non-directed *meta*-C–H activation. Substituted 2-pyridone ligands were found to be key in assisting the cleavage of the *meta*-C–H bond in the concerted metalation-deprotonation (CMD) process.

Graphical Abstract

yu200@scripps.edu.

[+]These authors contributed equally to this work.

Conflict of interest

The authors declare no conflict of interest.

Supporting information for this article is given via a link at the end of the document.

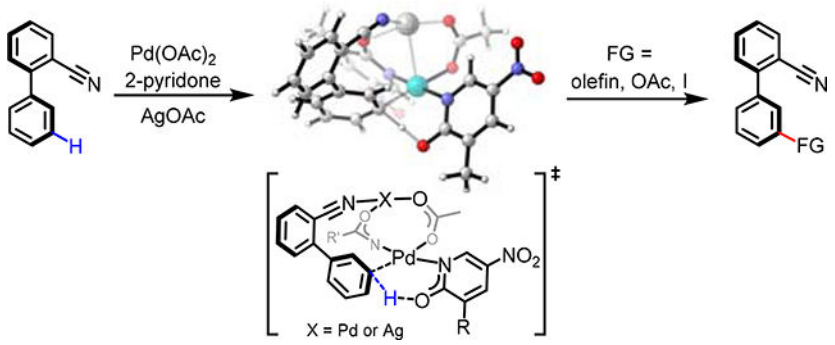

A nitrile-directed *meta*-C–H functionalization of biphenyl derivatives was realized through modifying 2-pyridone ligand. DFT calculations revealed a new ligand-containing Pd–Ag dimeric transition state is responsible for the *meta*-selectivity.

Keywords

biphenyl; C–H activation; remote; pyridone; Pd–Ag dimer

Introduction

Remote C–H bond activation/functionalization is essential for ultimately realizing molecular editing of organic structures through site-selective C–H functionalizations.[1] Previously, a number of approaches including electronic and steric effects have been exploited to achieve the site-selectivity of remote C–H activation of aromatic substrates.[2] In 2012, the Yu group has designed a nitrile-containing U-shaped template that directs remote *meta* C–H bonds of benzyl derivatives via a macrocyclophane-like palladated intermediate.[3] The combination of both distance and geometry was recognized as a very effective strategy to obtain the site-selectivity of remote C–H activation. We and others subsequently developed a number of U-shaped nitrile templates for *meta*- or *para*-selective C–H functionalization of aromatic alcohols, carboxylic acids and amines.[4]

Biphenyl derivatives have wide applications in ligand design as well as in pharmaceuticals.[5] Although a lot of biphenyl scaffolds have been synthesized via Suzuki coupling, however, presence of olefin moiety is not tolerated because of the competition and interference of Heck coupling. Due to the nitrile group is a transformable handle that can conduct a multitude of further transformations into an amine, acid, amide, ketone and heterocycle,[6] the use of readily available biphenyl nitrile substrates to direct remote C–H activation is a very powerful method for biaryl synthesis. In our previous work, we installed a U-template to afford *meta*-selective C–H functionalization of biaryl carboxylic acids (Scheme 1a).[3] Computational analysis showed that such design requires a molecular U-turn and a large ring size of the cyclophane transition state.[7] We compared the three possible Pd-containing transition state (TS) species: monomeric $Pd(OAc)_2$, dimeric $Pd_2(OAc)_4$ and heterodimeric $PdAg(OAc)_3$. Interestingly, the Pd–Ag heterodimeric species gave lower activation barriers for CMD C–H activation step.[7b–c] Encouraged by the computational heterodimeric transition state, we envisioned that the installed U-shaped template for the assembly of the

large sized cyclophane transition state may not be necessary for *meta*-C–H activation. Instead, the linear nitrile could coordinate to the dimeric transition metal and lead to a similar U-turn to reach the *meta* C–H bond. In this work, we use a 2-cyanobiphenyl substrate to compare the monomeric and dimeric transition states, and show that the Pd–Ag dimeric TS is predicted to give excellent *meta*-selectivity (Scheme 1b).

We report 2-pyridone ligand-promoted *meta*-selective C–H olefination, acetoxylation and iodination of the biaryl derivatives via Pd(II)/Pd(0) or Pd(II)/Pd(IV) catalysis (Scheme 1c). This approach avoids the design and installation of U-template to accomplish the high *meta*-selectivity. The modified 2-pyridone ligand improves the reactivity and gives moderate to good yields for all three transformations of biaryls. Computational studies reveal that the *meta*-selectivity resulted from the flexibility of a ligand-containing dimeric transition state structure. The free energy calculations for the *meta*-selective olefination pathway indicate that the CMD C–H activation step is the turnover-limiting step, which is also implied by the large experimentally found KIE values. Compared to the acetate pathway, the involvement of two 2-pyridone ligands gives lower energetic barriers in the all of steps of the mechanism.

Results and Discussion

Based on the computed Pd-Ag dimeric model involving simple phenyl nitrile, we began to investigate the feasibility of achieving remote *meta*-selective C–H olefination of 2-cyanobiphenyl (**1a**) with ethyl acrylate (**2a**) as the coupling partner (Table 1). We were pleased to find that under the reaction conditions of 10 mol% of Pd(OAc) and 3.5 equivalents of AgOAc in HFIP at 80 °C, the olefination product was isolated in 16% yield with the encouraging *meta*-selectivity (*meta*:others = 4:1). To enhance the reactivity and *meta*-selectivity, we added pivalic acid as the ligand; the yield and selectivity showed slight improvement. Then several additional type of pyridine or quinolone ligands (**L2-L4**)[8] developed by our laboratory were evaluated, but no significant acceleration of the reaction was observed. The poor *meta*-selectivity by **L4** is probably due to the strong sulfonic acid destroying the dimetallic bridge. Inspired by the fact that the MPAA ligand improves the *meta*-selectivity for the U-template directed C–H activation, we tested Ac-Gly-OH and other NHAc group containing bidentate ligands (**L6-L7**);[9] unfortunately, the *meta*-selectivity significantly decreased. We suppose that the bidentate ligands may change the angle of dimetallic bridge to activate the *ortho*- or *para*-C–H bond and give a mixture of olefination products. Recently, our group found that the 2-pyridone ligand is very powerful for assisting the C–H bond cleavage in the CMD process.[10] We propose that the aromatic skeleton of 2-pyridone is probably superior for stabilizing the Pd–Ag dimeric bridge and improving the reactivity and selectivity. A suite of commercial available 2-pyridone ligands (**L8-L20**) were investigated. To our delight, the addition of **L18** afforded *meta*-product **3a** in 61% yield and *meta*-selectivity was up to 6:1. To adjust the electronic property of 2-pyridone for further improving the reaction yield, several 3-alkyl-5-nitropyridone ligands (**L21-L27**) were synthesized. The experimental results showed that **L24** gave the best yield (73%) and selectivity (*meta*:others = 6:1).

To exclude the possibility of non-directed C–H olefination of arenes[10b] and to demonstrate the directing function of nitrile, we conducted several control experiments using other 2-

substituted biphenyls under the optimal conditions (Scheme 2). Replacing nitrile with the electron-withdrawing (NO_2 and CO_2Me) or electron-donating substituents (Me) gave no *meta*-selectivity, albeit with good yield for the olefination products. The results indicate that non-directed C–H olefination easily occurs in the presence of 2-pyridone ligand, but the *meta*-selectivity is hard to control by the electronic biases. Therefore, the directing effect of nitrile is critical for the *meta*-selectivity in the present catalytic cycle.

With optimized conditions for *meta*-C–H olefination in hand, we proceeded to investigate the scope of the reaction with biphenyl derivatives (Scheme 3). When electron-donating or -withdrawing substituents were attached to the nitrile-containing phenyls, the olefination reaction occurred smoothly and gave the desired products **3b-f** in good yields with high *meta*-selectivity. Because the *ortho*-substitution may contribute to the torsion of biphenyl about the joining single bond to form the favorable activation conformation, high yields and selectivity of **3g**, **3i**, **3q** and **3r** are observed. A broad range of *meta*- and *para*-substituents on the olefination phenyls are tolerated, providing the products in good yields. In the cases of *ortho*- or *para*-chloro-substituted substrates, the electronic biases decrease the yields of the corresponding products **3h** and **3p**, and give lower *meta*-selectivity. In contrast, *meta*-ester substituted biphenyl gave low yield for the desired product **3l** but the selectivity still favored *meta*-position. We surveyed the compatibility of the present *meta*-olefination on the complex natural product derivatives. The reactions were accomplished by treating with biphenyl-containing dihydrocholesterol and menthol derivatives. Despite low yields observed, likely due to steric hindrance, the *meta*-selectivity was good. These biologically active derivatives may provide more possibilities for drug discovery. We also evaluate the C–H olefination reaction on 1 mmol scale to synthesize *meta*-olefination product **3n**, which was purified on a silica gel column to give 71% isolated yield with 7:1 ratio for *meta*:others. The almost pure *meta*-product **3n** was obtained in 50% yield after recrystallization with EA/hexane and *meta*-selectivity is more than 20:1 via H^1 NMR analysis.

We next explored the scope of olefin coupling partners (Scheme 4). The acyclic or cyclic α,β-unsaturated esters underwent the olefination and gave the desired products **3u, 3v, 3z** and **3aa** in moderate to good yields with high selectivity. The geometry of the **3z** was determined to be *Z* configuration comparing the ^{1}H NMR analysis with the previous literature.[10b] The transformation was also suitable for α,β-unsaturated ketone and amide, albeit providing lower yields (**3w** and **3ab**). Interestingly, the olefins attaching with sulfonate and phosphonate afforded high yields and excellent *meta*-selectivity for the corresponding products **3x-y**.

Having established the feasibility of nitrile-directed *meta*-C–H olefination, we turned our attention to the use of the catalytic system to investigate other *meta*-C–H transformations. We first attempted to use Pd(II)/Pd(IV) catalysis to realize the *meta*-acetoxylation reaction under the nitrile-template directed *meta*-C–H oxidation conditions (Scheme 5).[4d–e] Fortunately, when the $PhI(OAc)_2/Ac_2O$ oxidation system was employed, the *meta*-oxidation product **6a** was isolated in 51% yield with 9:1 ratio of *meta*:others. The yield of **6a** significantly dropped in the presence of AgOAc as the oxidant, indicating no Pd–Ag dimeric complex was involved in this catalytic cycle. A variety of substitutions on different positions of biphenyl substrates were tested, giving the desired products **6b-g** in moderate yields with

good selectivity. We proposed that the Pd–Pd dimeric intermediate having higher activation barriers is less favorable than Pd–Ag species, which led to the lower reactivity of oxidation reaction than olefination. In order to accomplish diverse *meta*-selective transformations, we then studied the *meta*-C–H iodination reaction. As shown in Scheme 6, *meta*-C–H iodination reaction has been realized using *N*-iodosuccinimide (NIS) as iodinating reagent via Pd(II)/Pd(IV) catalysis.

To showcase the broad synthetic utility of biphenyl nitrile, the *meta*-functionalization products were converted to diverse functional groups (Scheme 7). The olefination product **3a** was firstly reduced to aliphatic motif **8**, which is more common in nature, and then the further reduction of **8** afforded a free amine and alcohol-bearing biphenyl **9**. The nitrile could be easily converted to amide **10** and ester **11** under basic or acidic condition, respectively. Remarkably, tetrazole derivative **12,** which owns the 2-biphenyl tertazole privilege skeleton of anti-hypertension Sartan drugs,[11] could also be generated in the presence of azide reagent.

Mechanistic experiments were conducted to support the proposed origins of *meta*-selectivity. We initially performed a D/H exchange experiment of deuterated substrate **[D_5]-1a** in the presence of 5 equivalents of water (Scheme 8a), but no protonated product as well as starting material was observed, supporting that the C–H bond cleavage is irreversible. Kinetic isotope effect (KIE) studies were also conducted (Scheme 8b). The intermolecular competition experiments provided a P_H/P_D value of 4.6 and parallel KIE was measured and the value of k_H/k_D was 2.6. These results indicate that C–H cleavage is probably the turnover-limiting step.[12]

We conducted the computational studies to understand how the *meta*-selectivity occurred, and why the 2-pyridone ligand promoted reactivity. Quantum mechanical calculations were performed with Gaussian 09.[13] Ground state and transition state geometries were optimized in the gas phase using the B3LYP-D3[14] functional with the 6–31G(d)[15] basis set for all nonmetal atoms and the LANL2DZ[16] basis set with effective core potential (ECP) for Pd. Single-point corrections were calculated using Truhlar's M06[17] functional with the 6–311++G(d,p)[18] basis set for all nonmetal atoms and the SDD[19] effective core potential for Pd. Single-point solvation energies were calculated by using SMD solvation model (solvent = generic, eps = 16.7, epsinf = 1.625625) to model HFIP. Vibrational frequencies were computed to determine if the optimized structures are minima or saddle points on the potential energy surface corresponding to minima and transition state geometries, respectively. The reported free energies include zero-point energies and thermal corrections calculated at 298.15 K and 1 atm. Molecular structures were illustrated with CYLview.[20]

First, we investigated the intrinsic optimized geometries of the 2-cyanobiphenyl substrate and a model system of a benzonitrile group coordinated to an Ag center (Figure 1). The substrate has a C_1–C_2–C_3–C_4 dihedral angle of 48°. The optimal C≡N–Ag angle of benzonitrile is 179°, showing that linear coordination to the metal center dictates a strong ligand binding.

In order to understand the origin of *meta*-selectivity, we investigated and compared several possible *ortho*-, *meta*- and *para*-selective CMD transition state structures involving a $Pd(OAc)_2$ monomer, a $Pd_2(OAc)_4$ dimer, and a $PdAg(OAc)_3$ heteronuclear dimer using an acetate ligand to assist CMD process (Figure 2). To our surprise, each model system was *meta*-selective. The Pd–Ag heterodimeric model gave an energetic barrier 5.7 and 10.0 kcal mol^{-1} lower than the Pd–Pd dimer and Pd monomer models, respectively. Our results are in accord with previous studies of Pd-catalyzed *meta*-selective C–H activation reactions[7b–c] where the longer intrinsic length of a Pd–Ag complex compared to a monomeric Pd complex accommodates a more favorable coordination of the 2-cyanobiphenyl substrate.

We found the 2-pyridone ligand gives an improvement of *meta*-selectivities. To explain the observation, we compared the free energies of 2-pyridone and acetate assisted CMD TS. To construct the 2-pyridone-containing TS, the first question is how many 2-pyridone ligands are coordinated to the metal centers at the CMD TS? In order to reduce computational burden, we use zero, one, two, and three 2-pyridone ligand **L18** instead of **L24** to compare the relative free energies of TSs. Interestingly, the CMD TS was lowest in energy when one **L18** bridged the Pd and Ag metal centers while another **L18** assist CMD. Using these calculations, we found the optimal $PdAgL_2(OAc)$ TS (Figure 3).

The detailed *ortho*-, *meta*- and *para*-selective $PdAgL_2(OAc)$ CMD transition states are shown in Figure 4. In the *ortho*-selective transition state structure, we found that the dihedral angle between carbons 1–4 is about 115°, but the dihedral angle of an optimized 2-cyanobiphenyl by itself is 48°. Also, the C≡N–Ag angle is 104°, which is far from an ideal ligand-to-metal coordination angle of 179°. This causes the Ag–N bond distance to increase to 2.45 Å. The *para*-selective TS shows similar characteristics to the *ortho*-TS where a longer N–Ag bond distance destabilizes the TS structure. But the *meta*-selective CMD TS has the lowest energetic barrier of 21.9 kcal mol^{-1}, and its dihedral angle between carbons 1–4 of 48° shows that the substrate has not been as distorted as seen in *ortho*- or *para*-TS structures. Also the N–Ag distance is much shorter, at 2.26 Å, indicating a stronger chelation to Ag, which stabilizes the TS. Also, the shorter C–H bond distance indicates an earlier transition state for *meta*-selectivity, which shows the ease of achieving the most favorable *meta*-TS structure.

We also analyzed the distortion energy at the transition state. To do this, we separated both the reactant complex and transition state structures into two parts: the substrate includes the 2-cyanobiphenyl with the proton undergoing CMD while the catalyst contains everything else in the system. We performed single point calculations of the two separated parts, the substrate and the catalyst, for reactant complex 1 and *meta*- selective CMD TS structure. Then we subtracted the energy of the substrate in the CMD TS from the energy of the substrate in the reactant complex to obtain the distortion energy of the substrate, E_{sub} (Figure 5). The same can be done to find the distortion energy of the catalyst E_{cat}, where this equals the energy of the catalyst in the CMD TS minus the energy of the catalyst in the reactant complex. To get the total distortion energy E_{total}, we add $E_{sub} + E_{cat}$ together and overall, we found that the total distortion of the *meta*-structure was the smallest in comparison to that of the *ortho*- and *para*-structures.

To demonstrate the 2-pyrdione ligand enhanced the reactivity, we used M06 for single point calculations in the free energy profile for the *meta*-pathway in the heterodimeric $PdAg(OAc)_3$ and $PdAgL_2(OAc)$ mechanisms. As shown in Figure 6, the $PdAgL_2(OAc)$ mechanism lowers the energy barriers of every step compared to the $PdAg(OAc)_3$ mechanism. Outside of the catalytic cycle, trimeric $Pd_3(OAc)_6$ dissociates into monomeric $Pd(OAc)_2$ and dimeric $Ag_2(OAc)_4$ dissociates into $Ag(OAc)_2$ Two pyridone ligands can displace two acetate groups to form the heterodimeric activated catalyst. The first key step is the CMD C–H activation in which one pyridone acts as a base to deprotonate the arene (**TS 1**), while a new Pd–C bond is formed, leading to **Int 2**. The second step is alkene insertion (**TS 2**) involving the olefin-coordinated palladacycle **Int 3** to form **Int 4**. The third step is β-hydride elimination (**TS 3**) where the hydride is transferred to Pd to form the **π**-complex **Int 5**. In the last few steps of the catalytic cycle, the palladium hydride intermediate **Int 5** undergoes product dissociation, reductive elimination to release the acetic acid, and oxidation of Pd^0 with the Ag^I oxidant to regenerate the Pd^{II} catalyst. There are several possibilities with the different orders of these steps. This process is expected to be highly exergonic and require low activation barriers. The details of these steps were not calculated. The calculation also shows C–H activation step suffers highest energy barriers in the whole mechanism, which is consistent with the KIE experimental results. We also added Grimme's dispersion corrections to our M06 single point calculations and found that there was no significant difference between the two reaction pathways (see Supporting Information).

Conclusion

We have developed methods for *meta*-C–H olefination, acetoxylation and iodination of 2-cyanobiphenyl derivatives via palladium/2-pyridone catalysis. The 2-pyridone ligand is critical for improving the reactivity and *meta*-selectivity. The reaction could be used to synthesize diversely substituted biaryls due to the versatile transformations of the simple phenyl nitrile. Though the nitrile is spatially and geometrically unfavorable to direct *meta*-C–H activation, DFT calculations proposed a nitrile assisted Pd–Ag dimeric transition state that favors the *meta*-selectivity. Among acetate, NHAc and 2-pyridone as proton acceptor in the CMD process, only 2-pyridone ligand could provide both good yields and highly *meta*-selectivity for these transformations. The computational results also indicated that one molecule of 2-pyridone and one acetate molecule participate in the bimetallic bridge to give the lower energy barriers. The computational dimetallic bridge mechanism opens a new avenue for other remote C–H activation reaction design.

Supplementary Material

Refer to Web version on PubMed Central for supplementary material.

Acknowledgements

We gratefully acknowledge The Scripps Research Institute (TSRI), the NIH (National Institute of General Medical Sciences grant R01 GM102265) and Bristol-Myers Squibb for financial support. We gratefully acknowledge Dr. Jason Chen (TSRI), Brittany Sanchez (TSRI), and Emily Sturgell (TSRI) for HRMS analysis. This work was also supported by the National Science Foundation (CHE-1764320 to KNH) and the National Science Foundation under the CCI Center for Selective C–H Functionalization (CHE-1700982). Computations were performed on the

Hoffman2 cluster at UCLA and the Extreme Science and Engineering Discovery Environment (XSEDE), which is supported by the NSF (OCI-1053575). K. L. B. thanks the Saul Winstein Fellowship (UCLA) for support.

References

[1]. a)Breslow R, Winnik MA, J. Am. Chem. Soc 1969, 91, 3083;b)Breslow R, Corcoran RJ, Snider BB, J. Am. Chem. Soc 1974, 96, 6791; [PubMed: 4414371] c)Breslow R, Acc. Chem. Res 1980, 13, 170.

[2]. For other examples of site-selective C–H activation, see:a)Zhang Y-H, Shi B-F, Yu J-Q, J. Am. Chem. Soc 2009, 131, 5072; [PubMed: 19296661] b)Cheng C, Hartwig JF, Science 2014, 343, 853; [PubMed: 24558154] c)Phipps RJ, Gaunt MJ, Science 2009, 323, 1593; [PubMed: 19299616] d)Yang Y, Li R, Zhao Y, Zhao D, Shi Z, J. Am. Chem. Soc 2016, 138, 8734; [PubMed: 27362919] e)Kuninobu Y, Ida H, Nishi M, Kanai M, Nat. Chem 2015, 7, 712; [PubMed: 26291942] f)Davis HJ, Mihai MT, Phipps RJ, J. Am. Chem. Soc 2016, 138, 12759; [PubMed: 27626468] g)Wang X-C, Gong W, Fang L-Z, Zhu R-Y, Li S, Engle KM, Yu J-Q, Nature 2015, 519, 334; [PubMed: 25754328] h)Dong Z, Wang J, Dong G, J. Am. Chem. Soc 2015, 137, 5887; [PubMed: 25909445] i)Saidi O, Marafie J, Ledger AE, Liu PM, Mahon MF, Kociok-Köhn G, Whittlesey MK, Frost CG, J. Am. Chem. Soc 2011, 133, 19298; [PubMed: 22047022] j)Hofmann N, Ackermann L, J. Am. Chem. Soc 2013, 135, 5877. [PubMed: 23534668]

[3]. Leow D, Li G, Mei T-S, Yu J-Q, Nature 2012, 486, 518. [PubMed: 22739317]

[4]. For examples of nitrile template-directed meta or para C–H activation, see:a)Dai H-X, Li G, Zhang X-G, Stepan AF, Yu J-Q, J. Am. Chem. Soc 2013, 135, 7567; [PubMed: 23614807] b)Lee S, Lee H, Tan KL, J. Am. Chem. Soc 2013, 135, 18778; [PubMed: 24325399] c)Wan L, Dastbaravardeh N, Li G, Yu J-Q, J. Am. Chem. Soc 2013, 135, 18056; [PubMed: 24236533] d)Tang R-Y, Li G, Yu J-Q, Nature 2014, 507, 215; [PubMed: 24622200] e)Yang G, Lindovska P, Zhu D, Kim J, Wang P, Tang R-Y, Movassaghi M, Yu J-Q, J. Am. Chem. Soc 2014, 136, 10807; [PubMed: 25007097] f)Bag S, Patra T, Modak A, Deb A, Maity S, Dutta U, Dey A, Kancherla R, Maji A, Hazra A, Bera M, Maiti D, J. Am. Chem. Soc 2015, 137, 11888; [PubMed: 26361337] g)Li S, Cai L, Ji H, Yang L, Li G, Nat. Commun 2016, 7, 10443; [PubMed: 26813919] h)Maji A, Guin S, Feng S, Dahiya A, Singh VK, Liu P, Maiti D, Angew. Chem. Int. Ed 2017, 56, 14903; Angew. Chem. 2017, 129, 15099;i)Modak A, Patra T, Chowdhury R, Raul S, Maiti D, Organometallics 2017, 36, 2418;j)Zhang L, Zhao C, Liu Y, Xu J, Xu X, Jin Z, Angew. Chem. Int. Ed 2017, 56, 12245; Angew. Chem. 2017, 129, 12413;k)Li M, Shang M, Xu H, Wang X, Dai H-X, Yu J-Q, Org. Lett 2019, 21, 540; [PubMed: 30615468] l)Xu H-J, Kang Y-S, Shi H, Zhang P, Chen Y-K, Zhang B, Liu Z-Q, Zhao J, Sun W-Y, Yu J-Q, Lu Y, J. Am. Chem. Soc 2019, 141, 76; [PubMed: 30585063] m)Xu J, Chen J, Gao F, Xie S, Xu X, Jin Z, Yu J-Q, J. Am. Chem. Soc 2019, 141, 1903. [PubMed: 30665300]

[5]. a)Welsch ME, Snyder SA, Stockwell BR, Curr. Opin. Chem. Biol 2010, 14, 347; [PubMed: 20303320] b)Wang Y-B, Tan B, Acc. Chem. Res 2018, 51, 534. [PubMed: 29419282]

[6]. a)Liskey CW, Liao X, Hartwig JF, J. Am. Chem. Soc 2010, 132, 11389; [PubMed: 20677758] b)Anbarasan P, Schareina T, Beller M, Chem. Soc. Rev 2011, 40, 5049. [PubMed: 21528150]

[7]. a)Cheng G-J, Yang Y-F, Liu P, Chen P, Sun T-Y, Li G, Zhang X, Houk KN, Yu J-Q, Wu Y-D, J. Am. Chem. Soc 2014, 136, 894; [PubMed: 24410499] b)Yang Y-F, Cheng G-J, Liu P, Leow D, Sun TY, Chen P, Zhang X, Yu J-Q, Wu Y-D, Houk KN, J. Am. Chem. Soc 2014, 136, 344; [PubMed: 24313742] c)Fang L, Saint-Denis TG, Taylor BLH, Ahlquist S, Hong K, Liu S, Han L, Houk KN, Yu J-Q, J. Am. Chem. Soc 2017, 139, 10702; [PubMed: 28749693] d)Yang Y-F, Hong X, Yu J-Q, Houk KN, Acc. Chem. Res 2017, 50, 2853. [PubMed: 29115826]

[8]. For examples of pyridine or quinolone ligand promoted C–H activation, see:a)He J, Li S, Deng Y, Fu H, Laforteza BN, Spangler JE, Homs A, Yu J-Q, Science 2014, 343, 1216. [PubMed: 24626923] b)Li S, Chen G, Feng C-G, Gong W, Yu J-Q, J. Am. Chem. Soc 2014, 136, 5267; [PubMed: 24666182] c)Li S, Zhu R-Y, Xiao K-J, Yu J-Q, Angew. Chem. Int. Ed 2016, 55, 4317; Angew. Chem. 2016, 128, 4389;d)Park H, Chekshin N, Shen P-X, Yu J-Q, ACS Catal. 2018, 8, 9292. [PubMed: 31223513]

[9]. a)Shen P-X, Hu L, Shao Q, Hong K, Yu J-Q, J. Am. Chem. Soc 2018, 140, 6545; [PubMed: 29741883] b)Zhuang Z, Yu C-B, Chen G, Wu Q-F, Hsiao Y, Joe CL, Qiao JX, Poss MA, Yu J-Q, J. Am. Chem. Soc 2018, 140, 10363. [PubMed: 30029574]

[10]. For examples of 2-pyridone ligand promoted C–H activation, see:a)Wang P, Farmer ME, Huo X, Jain P, Shen P-X, Ishoey M, Bradner JE, Wisniewski SR, Eastgate MD, Yu J-Q, J. Am. Chem. Soc 2016, 138, 9269; [PubMed: 27384126] b)Wang P, Verma P, Xia G, Shi J, Qiao JX, Tao S, Cheng PTW, Poss MA, Farmer ME, Yeung K-S, Yu J-Q, Nature 2017, 551, 489; [PubMed: 29168802] c)Chen Y-Q, Wang Z, Wu Y, Wisniewski SR, Qiao JX, Ewing WR, Eastgate MD, Yu J-Q, J. Am. Chem. Soc 2018, 140, 17884; [PubMed: 30500192] d)Zhu R-Y, Li Z-Q, Park HS, Senanayake CH, Yu J-Q, J. Am. Chem. Soc 2018, 140, 3564. [PubMed: 29481072]

[11]. Mavromoustakos T, Agelis G, Durdagi S, Expert Opin. Ther. Pat 2013, 23, 1483. [PubMed: 23968548]

[12]. Simmons EM, Hartwig JF, Angew. Chem. Int. Ed 2012, 51, 3066; Angew. Chem. 2012, 124, 3120.

[13]. Frisch MJ, Trucks GW, Schlegel HB, Scuseria GE, Robb MA, Cheeseman JR, Scalmani G, Barone V, Mennucci B, Petersson GA, Nakatsuji H, Caricato M, Li X, Hratchian HP, Izmaylov AF, Bloino J, Zheng G, Sonnenberg JL, Hada M, Ehara M, Toyota K, Fukuda R, Hasegawa J, Ishida M, Nakajima T, Honda Y, Kitao O, Nakai H, Vreven T, Montgomery JA, Peralta JE, Ogliaro F, Bearpark M, Heyd JJ, Brothers E, Kudin KN, Staroverov VN, Kobayashi R, Normand J, Raghavachari K, Rendell A, Burant JC, Iyengar SS, Tomasi J, Cossi M, Rega N, Millam JM, Klene M, Knox JE, Cross JB, Bakken V, Adamo C, Jaramillo J, Gomperts R, Stratmann RE, Yazyev O, Austin AJ, Cammi R, Pomelli C, Ochterski JW, Martin RL, Morokuma K, Zakrzewski VG, Voth GA, Salvador P, Dannenberg JJ, Dapprich S, Daniels AD, Farkas Ö; Foresman JB, Ortiz JV, Cioslowski J, Fox DJ, Gaussian 09; Gaussian Inc.: Wallingford, CT, 2009.

[14]. a)Becke AD, J. Chem. Phys 1993, 98, 5648;b)Lee C, Yang W, Parr RG, Phys. Rev. B: Condens. Matter Mater. Phys 1988, 37, 785;c)Becke AD, J. Chem. Phys 1993, 98, 1372;d)Stephens PJ, Devlin FJ, Chabalowski CF, Frisch MJ, J. Phys. Chem 1994, 98, 11623.

[15]. a)Ditchfield R, Hehre WJ, Pople JA, J. Chem. Phys 1971, 54, 724;b)Hehre WJ, Ditchfield R, Pople JA, J. Chem. Phys 1972, 56, 2257.

[16]. a)Hay PJ, Wadt WR, J. Chem. Phys 1985, 82, 299;b)Roy LE, Hay PJ, Martin RL, Chem J. Theory Comput. 2008, 4, 1029.

[17]. Zhao Y, Truhlar DG, Theor. Chem. Acc 2008, 120, 215.

[18]. Marenich AV, Cramer CJ, Truhlar DG, J. Phys. Chem. B 2009, 113, 6378. [PubMed: 19366259]

[19]. a)Dolg M, Wedig U, Stoll H, Preuss H, J. Chem. Phys 1987, 86, 866;b)Andrae D, Häussermann U, Dolg M, Stoll H, Preuss H, Theor. Chim. Acta 1990, 77, 123.

[20]. Legault CY, CYLview, 1.0b; Universitéde Sherbrooke, 2009 (http://www.cylview.org).

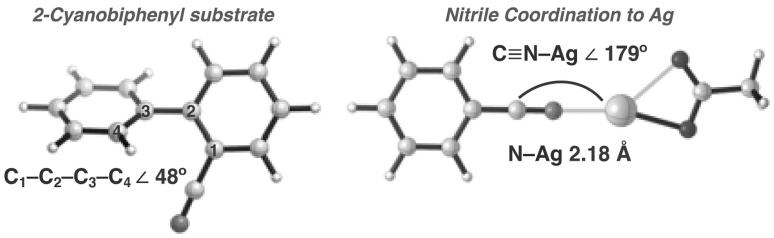

Figure 1.
Optimized geometries and angles (B3LYP-D3/LANL2DZ(Ag)/6–31g(d)).

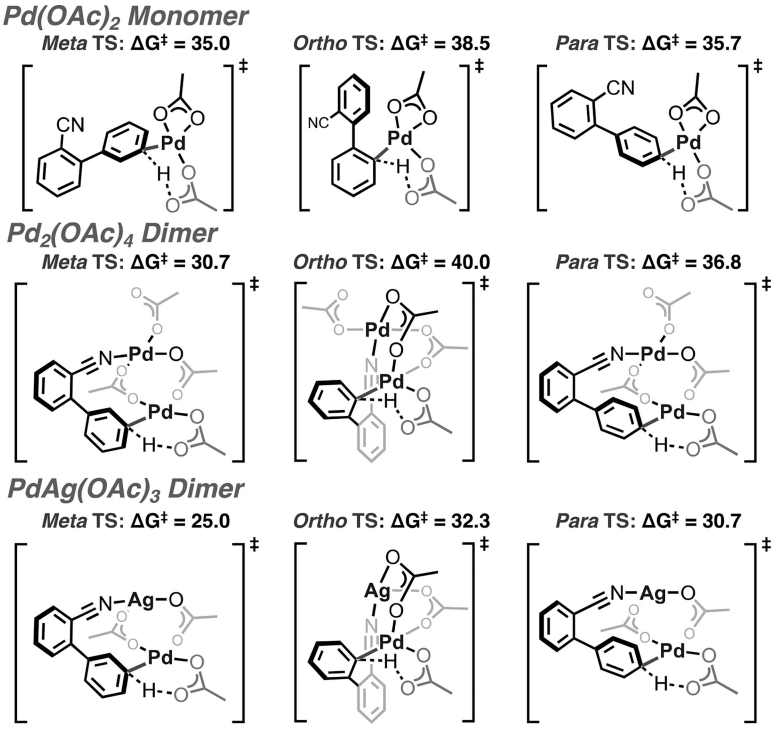

Figure 2.
Summary of CMD transition structures in the presence of an acetate ligand.

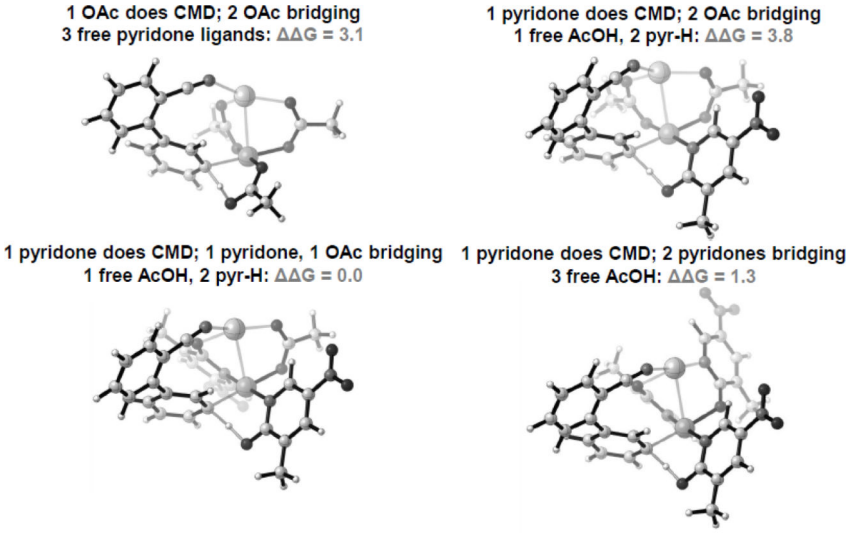

Figure 3.

Varying the number of **L18** at the $PdAg(OAc)_3$ *meta*-selective CMD transition state.

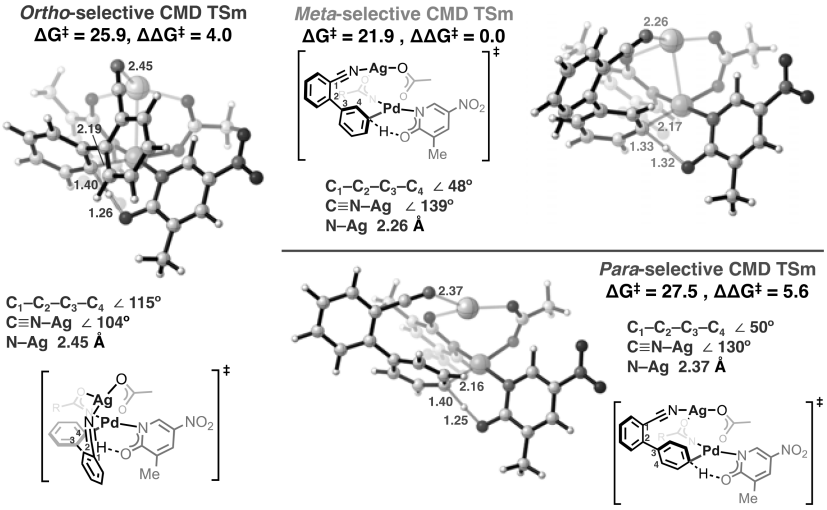

Figure 4.

$PdAgL_2(OAc)$ CMD transition state structures for *ortho*-, *meta*- and *para*-selectivities.

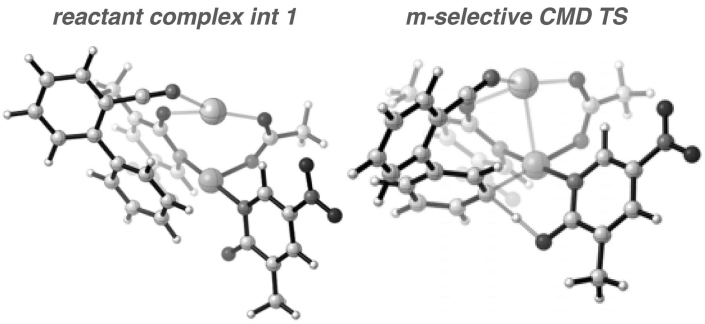

Distortion energy	*Meta* CMD TS	*Ortho* CMD TS	*Para* CMD TS
E_{cat} (kcal/mol)	1.2	3.3	3.6
E_{sub} (kcal/mol)	28.2	36.5	32.4
E_{total} (kcal/mol)	29.5	39.8	36.0

Figure 5.
Distortion analysis of the CMD TS involving two **L18**.

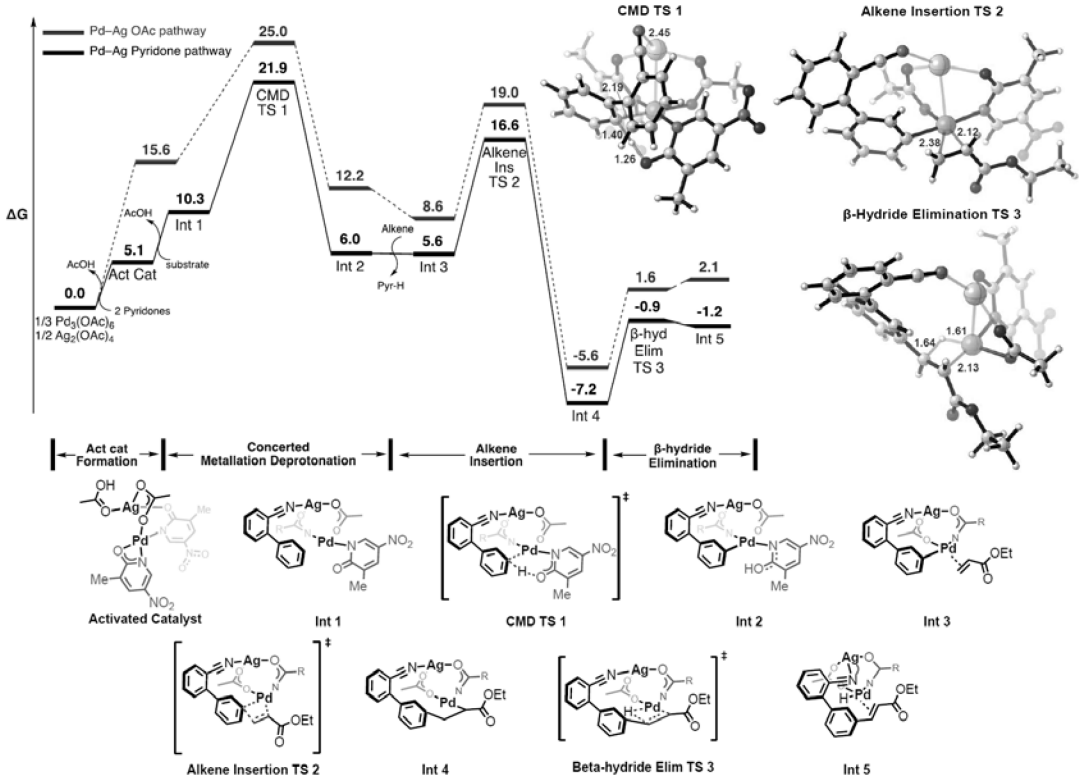

Figure 6.

Free energy profile for *meta*-selective C–H olefination of 2-cyanobiphenyl using SMD(Generic,eps=16.7,epsinf=1.625625)/M06/SDD(Pd)/6–311++G(d,p)//B3LYP-D3/LANL2DZ(Pd)/6–31G(d). Structures shown above correspond to the pyridone pathway.

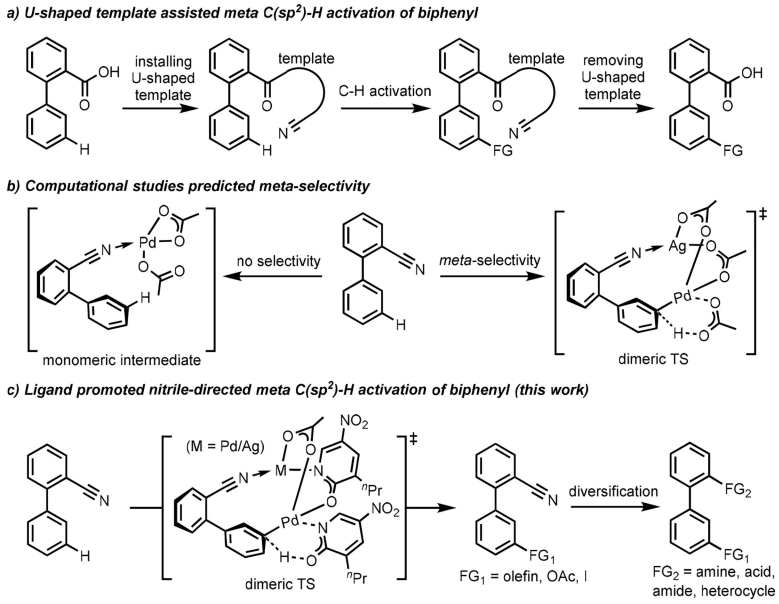

Scheme 1.

Rational development of *meta*-selective C–H functionalizations of biphenyls.

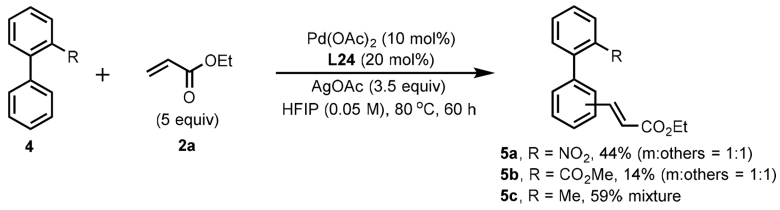

Scheme 2.
Control experiments.

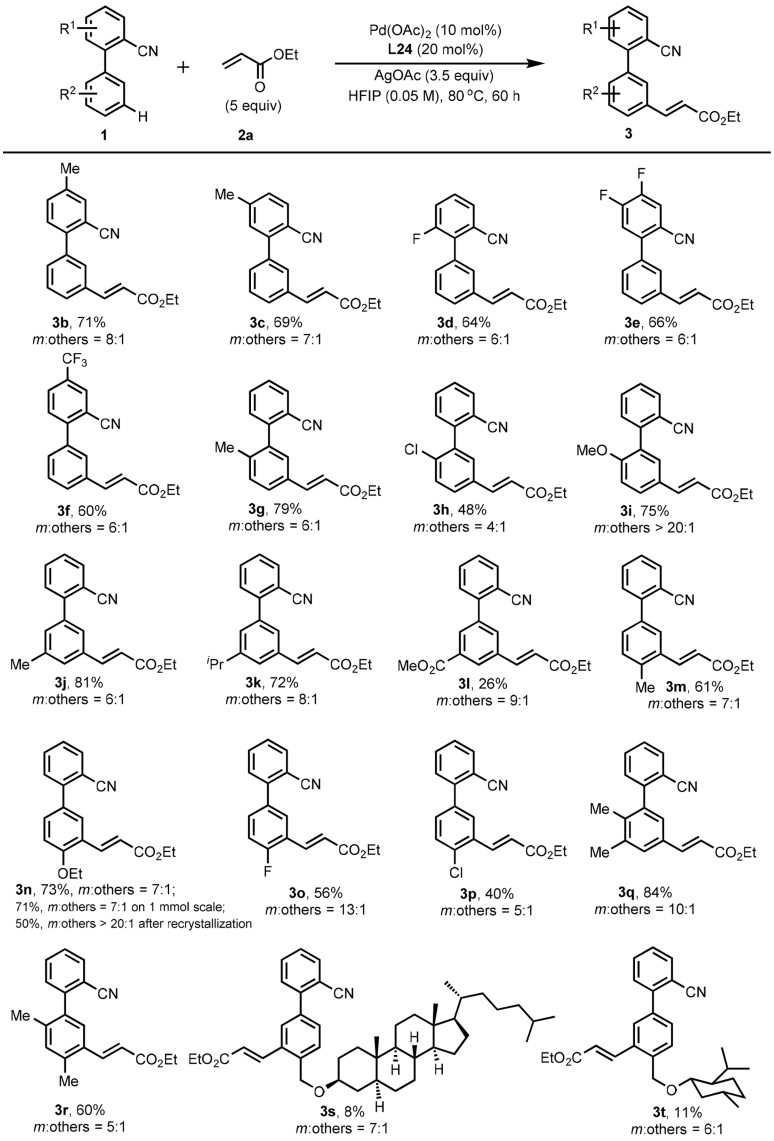

Scheme 3.

Substrate scope for *meta*-C(sp^2)–H olefination. [a] Reaction conditions: **1** (0.1 mmol), **2a** (5.0 equiv), $Pd(OAc)_2$ (10 mol%), **L24** (20 mol%), AgOAc (3.5 equiv), HFIP (2.0 mL), 80 °C, air, 60 h. [b] Isolated yields and the *meta*-selectivity was determined by GC-MS analysis (assisted with ^{1}H NMR analysis of the crude reaction mixture).

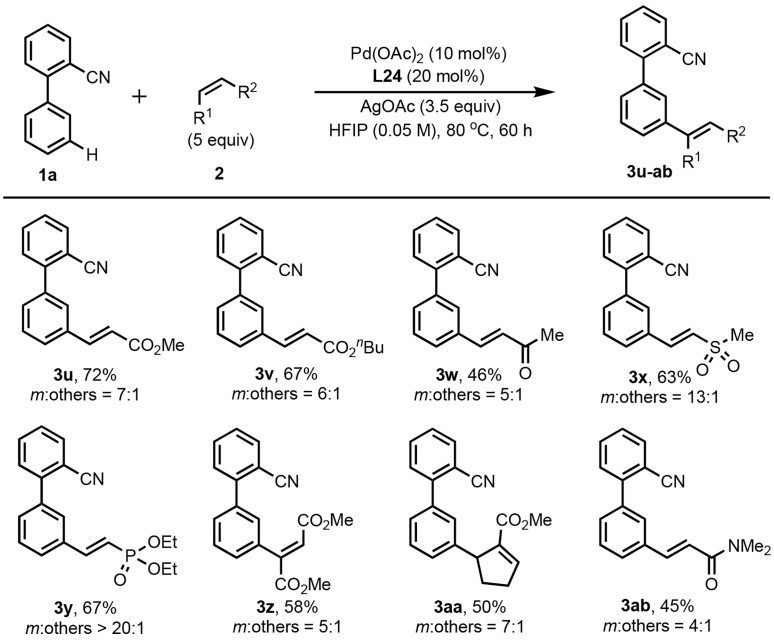

Scheme 4.

Olefin scope for *meta*-C(sp^2)–H olefination. [a] Reaction conditions: **1a** (0.1 mmol), **2** (5.0 equiv), $Pd(OAc)_2$ (10 mol%), **L24** (20 mol%), AgOAc (3.5 equiv), HFIP (2.0 mL), 80 °C, air, 60 h. [b] Isolated yields and the *meta*-selectivity was determined by GC-MS analysis (assisted with ^{1}H NMR analysis of the crude reaction mixture).

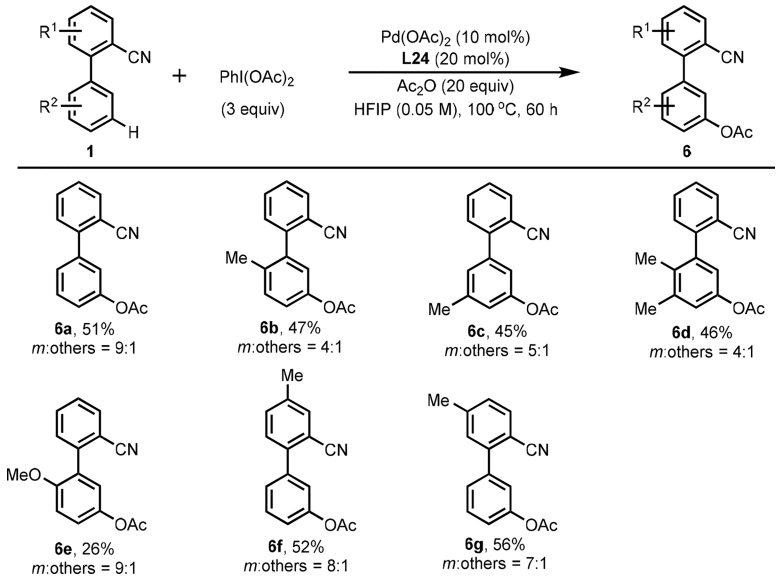

Scheme 5.

Substrate scope for *meta*-C(sp^2)–H acetoxylation. [a] Reaction conditions: **1** (0.1 mmol), $PhI(OAc)_2$ (3.0 equiv), $Pd(OAc)_2$ (10 mol%), **L24** (20 mol%), Ac_2O (20 equiv), HFIP (2.0 mL), 100 °C, air, 60 h. [b] Isolated yields and the *meta*-selectivity was determined by GC-MS analysis (assisted with ^{1}H NMR analysis of the crude reaction mixture).

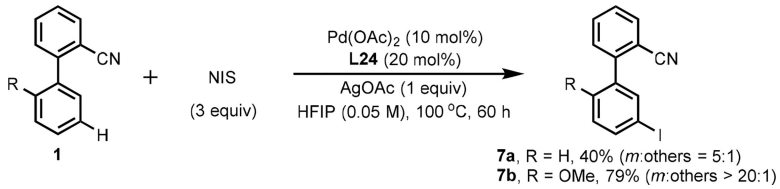

Scheme 6.

Representative examples for *meta*-C(sp^2)–H iodination. [a] Reaction conditions: **1** (0.1 mmol), *N*-Iodosuccinimide (3.0 equiv), $Pd(OAc)_2$ (10 mol%), **L24** (20 mol%), AgOAc (1 equiv), HFIP (2.0 mL), 100 °C, air, 60 h. [b] Isolated yields and the *meta*-selectivity was determined by GC-MS analysis (assisted with ^1H NMR analysis of the crude reaction mixture).

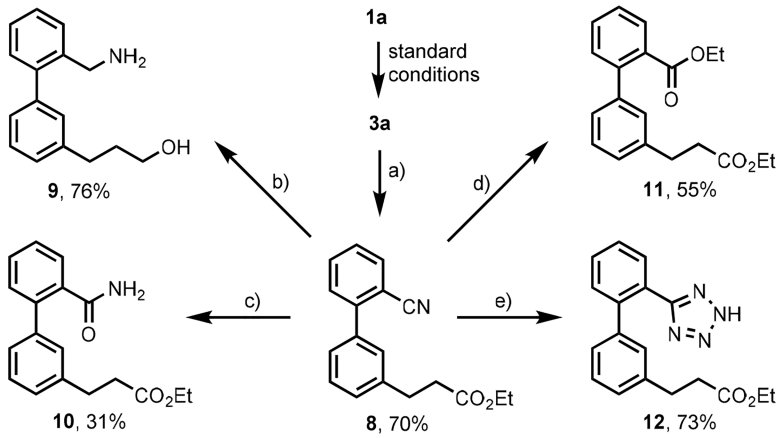

Scheme 7.

Diversifying transformations of nitrile directing group. a) Pd/C (20%), H_2, EtOH, 40 °C, 1 h; b) $LiAlH_4$ (6 equiv), Et_2O, rt, 5 h; c) 30% H_2O_2, K_2CO_3 (20 equiv), DMSO/H_2O, rt, 15 h; d) AcOH, H_2O/H_2SO_4, 120 °C, 6 h; after work-up, H_2SO_4 (5 drops), EtOH, 90 °C, 3 h; e) $TMSN_3$ (12 equiv), Bu_2SnO (0.3 equiv), toluene, 80 °C, 2 days.

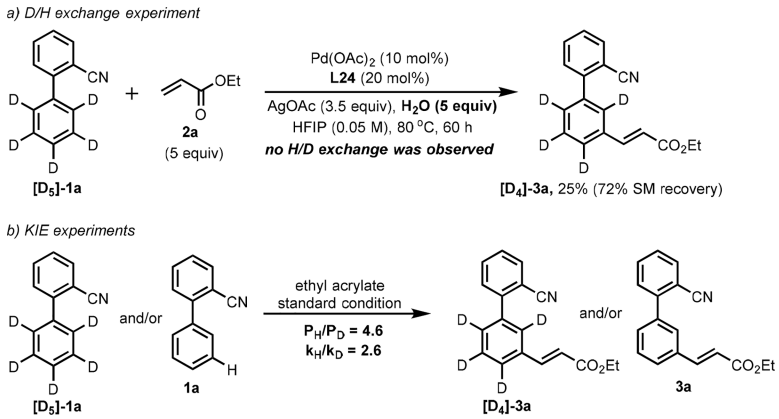

Scheme 8.
Preliminary mechanistic studies.

Table 1.

Ligand evaluation for *meta*-selective C–H olefination of 2-cyanobiphenyl.[a,b]

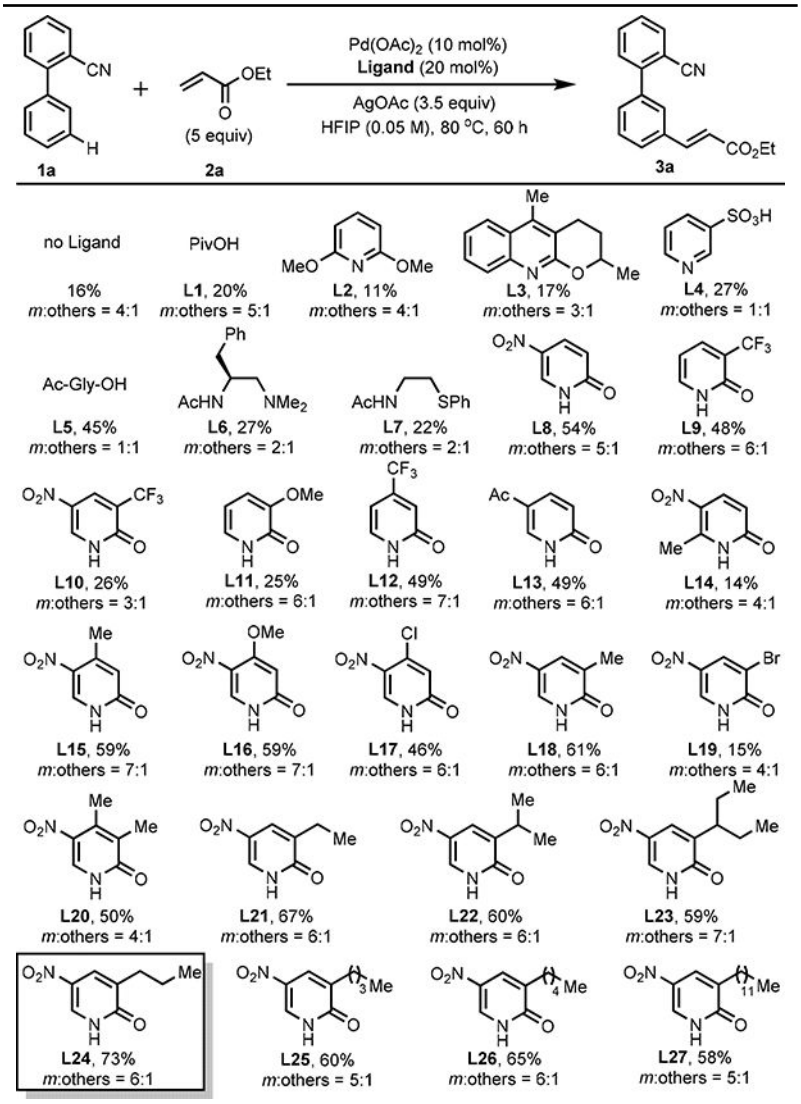

[a]Reaction conditions: **1a** (0.1 mmol), **2a** (5.0 equiv), $Pd(OAc)_2$ (10 mol%), ligand (20 mol%), AgOAc (3.5 equiv), HFIP (2.0 mL), 80 °C, air, 60 h.

[b]Isolated yields and the *meta*-selectivity was determined by GC-MS analysis (assisted with ^1H NMR analysis of the crude reaction mixture). HFIP = 1,1,1,3,3,3-Hexafluoro-2-propanol.